Science of the Total Environment 663 (2019) 867–877

Contents lists available at ScienceDirect

Science of the Total Environment

journal homepage: www.elsevier.com/locate/scitotenv

Decomposition of *Spartina alterniflora* and concomitant metal release dynamics in a tidal environment

Zhongzheng Yan *, Yan Xu, Qiqiong Zhang, Jianguo Qu, Xiuzhen Li

State Key Laboratory of Estuarine and Coastal Research, East China Normal University, Shanghai, China

HIGHLIGHTS

- The mass loss rate of the root and leaf decreased with the increase of burial time.
- The mass loss rate of the leaf and root was high in the high tidal marsh.
- Metals' concentration increased in leaf with the increasing of decomposition time.
- Pb isotope ratio in root litters decreased till the day 290 of decomposition.
- Pb isotope ratios in adjacent sediment had no significant changes.

GRAPHICAL ABSTRACT

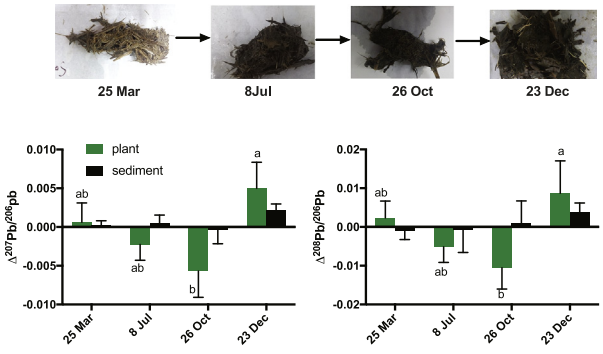

ARTICLE INFO

Article history:
Received 14 November 2018
Received in revised form 30 January 2019
Accepted 31 January 2019
Available online 1 February 2019

Editor: Filip M.G.Tack

Keywords:
Trace metals
Pb isotope
Decomposition
C/N ratio
Spartina alterniflora
Estuarine wetland

ABSTRACT

The decomposition of salt marsh plants is affected by the variation of physiochemical factors caused by the change of tide level. In the present study, plant tissues of *Spartina alterniflora* from controlled metal exposure experiments were subjected to a field decomposition trial at different tidal levels in a tidal flat of Chongming Island, Shanghai. The contents of the metals and Pb stable isotope ratios of the plant litter and the adjacent sediment were followed. The mass loss rate of the root and leaf litters of *S. alterniflora* decreased with the increase of burial time. Leaf had the highest decomposition rate (0.009 day^{-1} to 0.020 day^{-1}) compared to that of the roots (0.004 day^{-1} to 0.005 day^{-1}) and stems (0.002 day^{-1} to 0.006 day^{-1}). Leaf had the highest decomposition rate possibly due to the significantly lower C/N ratio (16.0–44.6) compared to that of the roots (32.8–88.9) and stems (43.7–120.9). The mass loss rate of the roots and leaves of *S. alterniflora* was higher in the high tidal marsh than that in the low tidal marsh, especially at the late stages of decomposition. The concentrations of metals in leaf litter of *S. alterniflora* increased, whereas the pools of metals in most of the plant litters decreased significantly with the increasing of the decomposition time. The ratios of $^{207}Pb/^{206}Pb$ and $^{208}Pb/^{206}Pb$ in the root litters decreased significantly in the first 290 days of decomposition and then increased significantly at Day 350, while the Pb isotope ratios in adjacent sediment showed no significant changes. Fast mass loss of plant litters induced the significant decrease in metals' pools at early stages of decomposition, and release of the plant tissue Pb was greatly inhibited due to the slowed mass loss at the late stages of decomposition.

1. Introduction

Trace metal pollution is among the most serious environment problems in coastal regions especially in estuarine wetlands (Idaszkin et al.,

* Corresponding author at: State Key Laboratory of Estuarine and Coastal Research, East China Normal University, 3663 Zhongshan Rd North, Shanghai, China.
E-mail address: zzyan@sklec.ecnu.edu.cn (Z. Yan).

https://doi.org/10.1016/j.scitotenv.2019.01.422
0048-9697/

2014; Sun et al., 2017). Salt marsh plants, such as *Spartina alterniflora* and *Phragmites australis*, can accumulate a large amount of trace metals in their roots, and a considerable amount of metals is transferred to the aboveground parts (such as leaves) (Windham et al., 2004; Weis and Weis, 2004). Salt marsh plants are thought to be the source of carbon (C) to the surrounding water and sediments during decomposition (Zawislanski et al., 2001). Decomposed salt marsh plant tissues, on the one hand, can becomes "sinks" for trace metals due to the adsorption and solidification of metals by the organic debris and microbes. On the other hand, trace metals in the tissues may be released to the sediments because of leaching and mineralization (Weis and Weis, 2004). In addition, some of the fixed trace metals are mobilized and released to the soil as metal "sources" due to the microbial activity (Gadd, 1993; Ledin, 2000). These metal "sources" might enter the high trophic levels and magnified through the detritus food chain and induce ecological safety problems in estuarine wetland ecosystems (Weis and Weis, 2004). Litter decomposition in intertidal zone is generally influenced by plant composition, the environmental factors, such as tidal flush, sediment temperature, and activities of the microbes (Weis and Weis, 2004; Lu et al., 2017; Sun et al., 2017).

To date, several studies are available on litter decomposition in estuarine wetland. Most of these studies focus on the litter mass loss during litter decomposition, the dynamics of some macro elements, such as C, nitrogen (N), and phosphorus (P), and the physiochemical and biological influencing factors (Liao et al., 2007; Zhang et al., 2014b; Guo et al., 2008; Gingerich et al., 2014). Some studies investigated the dynamics of accumulation and release of trace metals in the litters of marsh plants during decomposition (Breteler et al., 1981; Zawislanski et al., 2001; Weis and Weis, 2004; Du Laing et al., 2006; Lisamarie et al., 2010; Sun et al., 2016). Breteler et al. (1981) studied the dynamics of copper (Cu), zinc (Zn), chromium (Cr), and manganese (Mn) concentrations in the litters of *S. alterniflora* during degradation. They also found that the metal concentration increased significantly in the litters with increasing decomposition time, and the increase was suggested to be attributed to the metal-rich organic matter brought by tidal waves. Zawislanski et al. (2001) also found the concentration of trace metals increased obviously with the burial time of litter in the litter decomposition of five typical wetland plants in San Francisco Bay, and the increase of fine particles in litter bags was thought to be the direct cause of the increasing metal concentration. Significant accumulation of trace metals was also found in litters of *S. alterniflora* and *P. australis* during the decomposition and the cumulative rate of trace metals in the leaf litters was higher than in the stem (Lisamarie et al., 2010). Meanwhile, the metal pools (grams of metal per litterbag) of trace metals in the litters did not change significantly. Sun et al. (2016) found that Cu and Zn in the litters of three wetland species, *P. australis*, *Suaeda salsa*, and *Suaeda glauca*, increased significantly, whereas the total amount of Pb decreased compared with the initial degradation value. In summary, the accumulation and release of trace metals in litter decomposition is a very complicated process, and the changes of the concentration or the pool of trace metals may vary with plant species, plant part and metal type. There are three underlying processes that govern the changes of concentration and pool of trace metals in the plant litter: 1) metal's concentrating induced by the degradation of plant tissue, 2) adsorption of organic complex containing metals, and 3) loss of metals due to the decay of plant tissue (Breteler et al., 1981). In the above processes, the exchange of trace metals between plant tissues and sediments, as well as the final fate of trace metals in plant litters are still unclear.

Among the common trace metals in the estuarine wetland sediment, Pb is more stable than the other metals such as Cu, Fe, Mn, Cr and Hg. This is because the valent state of Pb is recalcitrant to the influence of the redox potential change or the microbial activities in the sediment (Du Laing et al., 2009; Young, 2013). The stability of Pb makes it an ideal representative for studying the exchange of trace metals between plant tissues and adjacent sediments during the decomposition of plant tissues. Pb has four stable isotopes, namely, ^{204}Pb, ^{206}Pb, ^{207}Pb, and ^{208}Pb, in which ^{206}Pb, ^{207}Pb, and ^{208}Pb are produced by the radioactive uranium and thorium. The ratio of these stable isotopes to environmental samples (soil, sediments, atmospheric particulates, and organic matters) is often used to identify the sources of Pb (natural or human activity) (Yang et al., 2007). In recent years, some researchers studied the source of Pb in estuarine wetland environment and biological samples via the Pb isotope tracer method (Caetano et al., 2007; Notten et al., 2008). However, the Pb stable isotope analysis of litter and environmental sediment during litter decomposition is still rare. The plant grown under the artificial Pb exposure at controlled experiments must have different stable Pb isotope fingerprints compared with those of the natural environmental sediments. We hypothesized that changes of Pb isotopes ratios in the artificial Pb-enriched plant sample should be different from that of the adjacent sediments during the decomposition process. By following the relative changes of the trace metals and Pb isotopes ratios of these two parts, an in-depth understanding on the exchange of trace metals between the marsh plant litters and the sediments can be achieved. The present study, therefore, aimed to investigate the changes of trace metal concentrations and metal pools in marsh plant litters during decomposition under tidal flat conditions. Pb isotope fingerprint of the plant litters and sediments was also followed to look into the exchange of trace metals between the plant litters and the sediments. *S. alterniflora*, a typical perennial estuarine marsh plant, was used as the experimental object (Li et al., 2009).

2. Materials and methods

2.1. Experimental setup

The sample burial site was set in the estuarine wetland of north Chongming Island according to the accessibility of the traffic and the convenience of the experimental operation (Fig. 1). Three tidal positions (low, middle, and high) were set along a transect at different distances from the tidal creek, and three parallel positions were selected at each tidal position with a space interval of 5 m. The low tidal position was spaced 100 m apart from the tidal creek. The middle tidal position was spaced 178 m apart from the low tidal positions, and the high tidal position was spaced 320 m apart from the middle tidal positions. The relative elevation of the tidal flat of different sites was measured by a total-station electronic tacheometer (Model GPT-102R, Shanghai Tongtai Mapping Service Co., Ltd., China), in which the high tidal position was −1.40 m, middle tidal position was −1.9 m, and the low tidal position was −2.00 m.

Buried samples of *S. alterniflora* were obtained from controlled metal (Cu, Zn, Pb, and Cr) exposure experiments (Xu et al., 2018). For the metal exposure treatment, the treatment solution was prepared by dissolving appropriate amounts of $CuCl_2$, $ZnCl_2$, $PbCl_2$, and $CrCl_3$ in salt water (10‰ NaCl) to achieve the final concentrations of 23.4, 60.8, 18 and 11.2 mg L^{-1} for Cu^{2+}, Zn^{2+}, Pb^{2+}, and Cr^{3+}, respectively. All chemicals used in the culture experiments were analytically pure. After 60 days culture, the plants were collected and rinsed with deionized water, after which they were separated into the roots, stems, and leaves. Then, different parts of the plants were oven-dried at 70 °C for 2 days. Subsequently, the samples were cut with scissors and homogenized and then separated into different aliquots with dry weight of 7.0, 10.2, and 5.2 g for the root, stem, and leaf, respectively. The weight plant samples were placed in a 20 × 20 cm nylon mesh bag (2 mm mesh).

In estuarine wetland of Shanghai, dead plant tissues of *S. alterniflora* were always found to be buried by the sediments due to the falling over of the plants and the harvesting activities in fall. In order to investigate the decomposition of the buried plant tissues and the variation of metals in the tissues, we buried the sealed nylon net bags at the parallel positions (triplicates) of all the tidal level as shown in Fig. 1, and the burial depth was approximately 5 cm. To avoid the loss of the mesh bags due to the tide washing, the bags were tied on polypropylene

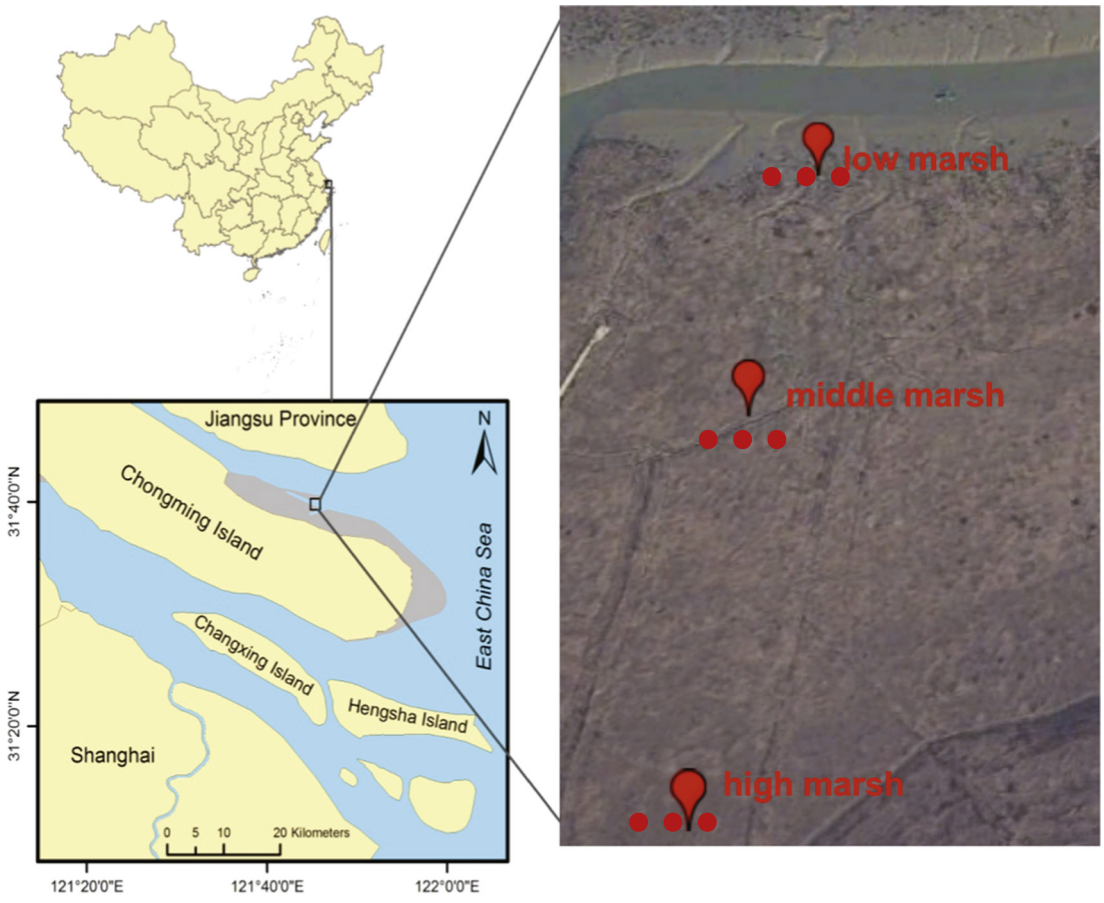

Fig. 1. Location of the experimental site.

tent pegs inserted into the sediments. The burial of the samples was started from 4 January 2017 and ended on 23 December 2017, which lasted 350 days. The mesh bags were collected at four time points, as follows: 25 March 2017 (Day 81), 8 July 2017 (Day 184), 26 October 2017 (Day 290), and 23 December 2017 (Day 350). At each sampling time, the adjacent sediments were collected and brought to the laboratory for future analysis.

The remaining samples in the mesh bags were carefully rinsed with deionized water and oven-dried at 70 °C for 2 days. The dry weight of litters was recorded. The dried plant litters were then homogenized with a ball grinding mill and stored in Ziplock bags to measure the carbon to nitrogen ratio (C/N ratio), lignin and cellulose content, metal (Cu, Pb, Zn, and Cr) concentrations, and the Pb isotope ratios of $^{207}Pb/^{206}Pb$ and $^{208}Pb/^{206}Pb$. The collected sediment sample was ground with a mortar and pestle and sieved through a 100-mesh sieve. The homogenized sediment samples were also stored in a Ziplock bag to measure the physiochemical properties, metal content, and Pb isotope ratios.

2.2. Measurements

2.2.1. Litter mass loss during decomposition

The litter mass loss (R, %) of different plant parts were calculated according to the equations of Olson (1963), as follows:

$$R = \frac{(W_0 - W_t)}{W_0} \times 100\%,$$

where W_0 (g) is the original dry mass of the litter, and W_t (g) is the dry mass of the litter at the time of collection.

Litter decomposition rates were calculated by the first-order decomposition model (Olson, 1963; Simões et al., 2011):

$$\frac{L_t}{L_0} = e^{-kt},$$

where L_t is the litter dry mass remaining after t days of decomposition. L_0 is the litter initial dry mass. k is the exponential breakdown coefficient. t is the days of decomposition.

2.2.2. Metals in plants and in sediments

The concentration of metals in plant litters and sediments was determined by the wet digestion method. Approximately 0.2 g of the dried plant tissue was digested in a polyfluortetraethylene (PTFE) beaker with 10 mL nitric acid, 5 mL hydrofluoric acid, and 5 mL perchloric acid. The PTFE beaker was heated on an electric hot plate for 3 h at 200 °C. During digestion, the lid of the PTFE beaker was kept covered to avoid the splashing of the digest. After digestion, the remnant in the beaker was dissolved and washed thrice with 5 mL of 1% nitric acid. The washes were combined and mixed with deionized water to make 25 mL in a volumetric flask. The concentrations of Cu and Zn in the digests of treatment solutions and sediments were analyzed by flame atomic absorption spectrometry (AAS, AAnalyst800, Germany). Pb and Cr were determined by inductively coupled plasma atomic emission spectroscopy (ICAP-7400, Thermo Fisher Inc. USA). Certified reference material of the carrot (GBW10047) and soils (GBW 07410) from the China National Center for Standard Materials were used for quality control. The averaged recovery rates for Cu, Zn, Pb, and Cr in GBW10047 were 127.5 ± 14.5%, 90.2 ± 5.4%, 98.2 ± 13.9%, and 88.7 ± 11.8%, respectively. The average recovery and the standard error (SD) of Cu, Zn, Pb, and Cr in GBW07410

were 96.3 ± 0.7%, 114.0 ± 8.0%, 87.1 ± 3.4%, and 83.5 ± 1.7%, respectively.

The accumulation and release of metals in the litters were evaluated by calculating the metal accumulation index (AI) according to the method of Sun et al. (2016), as follows:

$$AI = \frac{M_t \times C_t}{M_0 \times C_0} \times 100\%,$$

where M_0 is the original dry mass of the plant litters. C_0 is the original metal concentration of the litters. M_t is the dry mass at the sampling time "t." C_t is the metal concentration at sampling time "t."

2.2.3. Pb isotopes

Before the determination of Pb isotopes in samples, the total Pb content in the digestion solution of the plant and sediment samples were determined by AAS. The digestion solution was then diluted with 2% ultrapure nitric acid solution to approximately 25 μg L^{-1} in accordance with the Pb content. The ratio of $^{208}Pb/^{206}Pb$ and $^{207}Pb/^{206}Pb$ in the diluent was then determined using a high-resolution inductively coupled plasma mass spectrometer (Element 2, Thermo Finnigan, Germany). The National Institute of Standards' Lead Standard Reference Material (NIST SRM 981) was used as an external standard for calibration. During the measurement, the NIST 981 standard solution was calibrated every after four samples were measured for correction of mass discriminatory effects and drift of instrument parameters. Among them, the $^{208}Pb/^{206}Pb$ reference value in NIST 981 was 2.1681 ± 0.0008. The $^{207}Pb/^{206}Pb$ reference value was 0.91464 ± 0.000033.

2.2.4. Lignin and cellulose content of the plant materials

Lignin content in plant materials was determined according to the method of Syros et al. (2004). Dried plant materials (40 mg) was placed in a test tube, and the samples were first extracted by 3 mL of 80% ethanol for 1.5 h in a water bath at 80 °C. Then, the samples were extracted by 3 mL of chloroform at 62 °C for 1 h. The samples were subsequently dried at 50 °C for 2 days. The dried samples were digested in 2.6 mL digestion solution containing 25% (v/v) acetyl bromide (in acetic acid) and 2.7% (v/v) perchloric acid. After 1 h, 100 μL of the digest was combined with 580 μL of a solution containing 17% (v/v) 2 mol L^{-1} sodium hydroxide and 83% (v/v) acetic acid and 20 μL of 7.5 mol L^{-1} hydroxylamine hydrochloride. The final volume was corrected to 2 mL with acetic acid, and the absorbance at 280 nm was recorded. Lignin (analytically pure from Sigma) was used as the standard to quantify the lignin content in the samples.

Cellulose content was measured according to the method of Niu et al. (1992). Approximately 20 mg each of the root, stem, and leaf samples was weighed into a 15 mL caped centrifuge tube and mixed with 15 mL of ice-cold 60% H_2SO_4. The mixture was digested in an ice-bath for half an hour. The digest was shaken thoroughly and then filtered with a glass crucible funnel. Then, 1 mL of the above filtrate was diluted to 10 mL with deionized water. Subsequently, 2 mL of the diluted solution was mixed with 0.5 mL of 2% fluorenone reagent (prepared in ethyl acetate) and 5 mL of 60% H_2SO_4. The mixture was kept in boiled water bath for 10 min and then quickly cooled in a refrigerator. The absorbance of the mixture was measured at a wavelength of 620 nm by using a spectrophotometer (UV–1800PC, Mapada, Shanghai). Cellulose (analytically pure from Sigma) was used as the standard to quantify the cellulose content in the samples.

2.2.5. Sediment physiochemical characteristics

During the sampling of plant samples, the Eh values of the rhizosphere sediments were measured in situ with an Oxidation Reduction Potential meter (Spectrum IQ150, Spectrum Technologies Inc., USA). To measure the sediment salinity, 8 g of the air-dried soil samples was dissolved in deionized water at a ratio of 1:5 (w/v) and then filtered with filter paper. The electric conductivity (EC) of the filtrate was determined with an electric conductivity meter (Model CT-3031, Xi'an Yingheng Instrument Co., Ltd., China) and then converted into salinity (‰) by the empirical formula between EC and salinity:

$$Salinity\ (‰) = \frac{(0.5095 \times EC - 0.0841) \times V}{DW},$$

where EC is the electric conductivity of the filtrate, V is the volume of the water that used to dissolve the sediment samples, and DW is the dry weight of the sediment samples.

Total organic matter (TOM) was estimated by the classic Loss-On-Ignition method (Heiri et al., 2001). In brief, the sediment samples were first oven-dried at 105 °C overnight, cooled in a desiccator, and weighed before combusting at 550 °C for 6 h in a muffle furnace. After combustion, the samples were cooled in a desiccator and reweighed. The TOM content of the sediments was calculated using the following equation:

$$TOM(\%) = \frac{W_{bc} - W_{ac}}{W_{bc}} \times 100\%,$$

where W_{bc} and W_{ac} are the sediment weights before and after combustion, respectively. The texture of the sediment (relative contents of clay, slit, and sand) and median diameter of the sediments were analyzed with a laser diffraction particle size analyzer (Model LS™ 13 320, Beckman Coulter Inc., USA).

2.3. Statistical analysis

The mean and standard deviations of the three replicates for each treatment were calculated. All data passed the Shapiro-Wilk test, indicating that all data follow a normal distribution. Parametric one-way ANOVA and post-hoc multiple comparison (Turkey's test) were also conducted to determine the significant differences in different parameters under different waterlogging time treatments and tidal positions. A two-way multivariate analysis of variance (MANOVA), with tidal levels and the decomposition time as the two fixed factors, was applied to examine any significant interactive effects and differences in the decomposition rate (R) of the different parts of *S. alterniflora* and different variables. Statistical analyses were performed via SPSS version 16.0.

3. Results

3.1. Mass loss during the decomposition

The exponential breakdown rates (k value) of the leaf of *S. alterniflora* at high marsh flat ranged from 0.009 day^{-1} to 0.020 day^{-1}. These values were significantly higher than that at low and middle marsh flats. The k value of root ranged from 0.004 day^{-1} to 0.005 day^{-1} and was the highest in high marsh flat. The k value of stem ranged from 0.002 day^{-1} to 0.006 day^{-1} and showed no significant variations at different tidal positions (Fig. 2). At Day 81, out of the different parts, the stem showed the least mass loss (16.7%–19.1%), whereas the leaf had the highest mass loss (45.9%–53.8%). The different tidal levels showed no significant differences in mass loss of the root and stem at Day 81, whereas the mass loss of the leaf in high marsh is significantly higher than that in the middle marsh (Fig. 3). At Day 184 of the decomposition, the majority of the leaf litters mass were lost (79.2%–87.7% of the initial mass), whereas the mass loss of the root and stem was far below the mass loss of leaf (Fig. 3). With increasing decomposition time, similar trends were observed in the mass loss of different plant parts, i.e., the litter mass loss was high in the high marsh and low in the low or middle marsh. At Day 350, 95.6%–99.8% of the leaf litters and 70.3%–84.6% of the root litters were lost, and the rate for stem litters was 56.8%–82.2%. Two-way MANOVA results indicated that the tidal levels and decomposition time all had significant effects on the mass loss of different plant parts during the decomposition

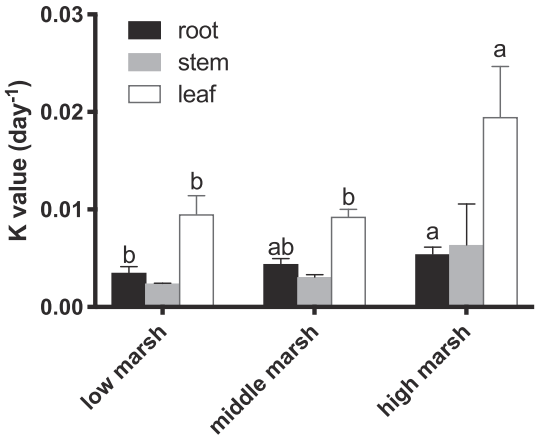

Fig. 2. Litters exponential breakdown coefficient (k) of different part of *S. alterniflora* at different tidal levels (values are mean and SD; for each parameter, data with different letters are significantly different at $p \le 0.05$).

Table 1
Two-way MANOVA results showing the effects of tidal levels and decomposition time and the interaction between these two sources of variations (df, Degrees of freedom; M.S., mean sum of squares; Sig: significance).

Source	Sources of variations	df	Mean square	F	Sig.
Tidal	Root R	2	402.266	18.559	0.000
	Stem R	2	865.420	24.735	0.000
	Leaf R	2	118.125	21.023	0.000
Time	Root R	3	4951.109	228.422	0.000
	Stem R	3	4280.142	122.331	0.000
	Leaf R	3	4535.399	807.184	0.000
Tidal * time	Root R	6	41.089	1.896	0.123
	Stem R	6	143.956	4.114	0.006
	Leaf R	6	18.106	3.222	0.018

(Table 1). Tidal levels and the decomposition time had significant interactive effects on the mass loss of the stems and leaves (Table 1).

3.2. Changes in C/N ratio and the content of lignin and cellulose

Fig. 4A shows the C/N ratio of different parts of *S. alterniflora* during decomposition. At the beginning of the experiments, the C/N ratio of the root and stem was roughly equal and higher than that of the leaves. With increasing decomposition time, C/N ratio decreased in the roots but increased significantly in the stems and leaves at Day 81. This outcome resulted in a significantly higher ratio in the stem than in roots. The root C/N ratios kept decreasing until Day 184, whereas the ratio in the stems and leaves further decreased until Day 290.

The lignin content in the litters of different parts of *S. alterniflora* had no significant changes during the first 184 days after burial (Fig. 4B). After Day 184, the lignin contents of all plant parts increased significantly at Day 290 and leveled off till the end of the experiment (Fig. 4B). The cellulose content in the litters of different parts of the plant generally showed decreasing patterns with the increasing of decomposition time (Fig. 4C). In the roots and stems, significant decreases in cellulose content were only observed at the last sampling time (Day 350). In comparison, the significant decrease in cellulose content in leaf litters was observed at Days 81, 290, and 350.

To study the influencing factors of litter decomposition, the mass loss rate of each part of the *S. alterniflora* was correlated with the content of lignin and cellulose and C/N ratio (Table 2). A significant positive correlation was found between the root mass loss rate and C/N ratio ($r = 0.802$, $p < 0.01$) and cellulose ($r = 0.640$, $p < 0.05$). The mass loss rate of the leaves was negatively correlated with the lignin content ($r = -0.774$, $p < 0.01$) and positively correlated with leaf C/N ratio ($r = 0.941$, $p < 0.01$). No significant correlation was observed among stem mass loss and lignin, C/N, and cellulose contents.

3.3. Variation of metal concentration in plant tissues

Fig. 5 shows the concentrations of different metals in litters of *S. alterniflora* at different burial stages. Increasing in Cu concentration in the root litters was observed at different burial stages, and significant increases were observed at Days 184 and 350 (Fig. 5A). Zn in root litters had no significant changes during the decomposition (Fig. 5B). The concentration of Pb and Cr in root litters showed similar trends and increased at early stages of the decomposition and decreased with increasing burial time (Fig. 5C and D). In stem litters, the changes in the concentration of Cu, Zn, and Pb showed similar trends, which decreased at the first sampling and showed no significant change until the end of the burial experiment (Fig. 5A, B, and C). The Cr concentration increased significantly in stem litters at the late burial stages (Fig. 5D). The concentration of all four metals showed similar trend in the leaf litters along the different burial stages but increased with the prolonging of burial time. Significant increases were also observed at the late stages of the decomposition.

During litter decomposition, the content of metals, especially Zn, Pb, and Cr, in sediments increased considerably compared with the original value (Fig. 5E). Table 3 shows the variation of sediment physiochemical parameters during the burial experiment. Salinity of the sediments roughly increased with the increasing of burial time, and the highest levels were recorded on 23 December 2017 (Day 350). TOM of the sediments also increased significantly from 4 Jan (Day 1) to 23 December 2017 (Day 350). The adjacent sediment Eh value showed a striking contrast at the late stage of decomposition, and the sediments on Day 290 was far more reductive than that on Day 350. Pearson correlation analyses showed that the increased accumulation of metals in the sediments

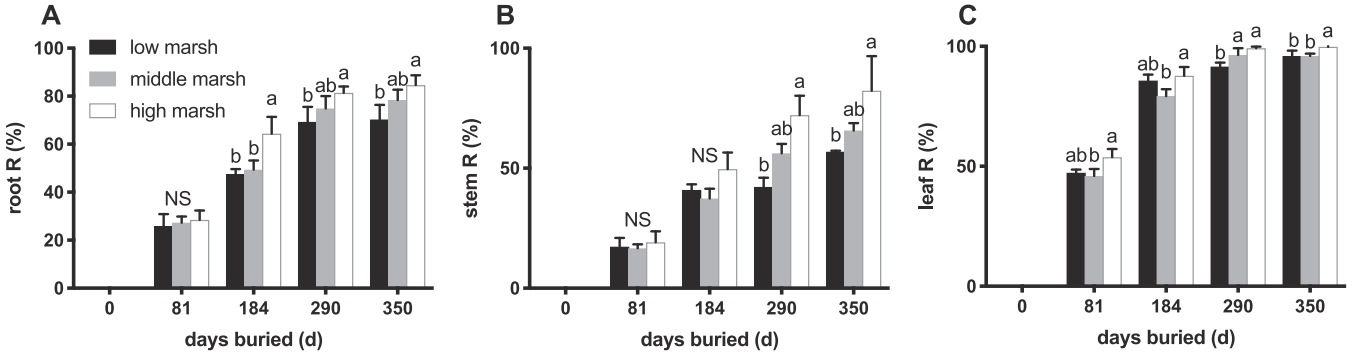

Fig. 3. The litter mass loss (R, %) of different plant parts of *S. alterniflora* at different time of decomposition (values are mean and SD; for the tidal levels at different time, data with different letters are significantly different at $p \le 0.05$; NS, not significant).

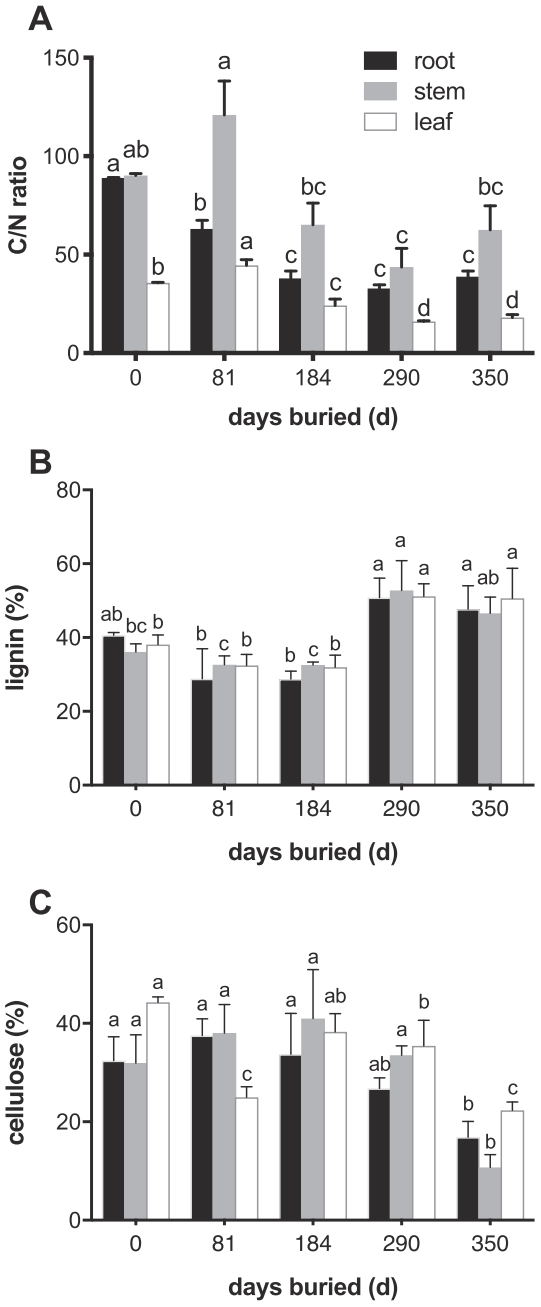

Fig. 4. Changes of litter (A) C/N ratio, (B) lignin content and (C) cellulose content in different parts of *S. alterniflora* at different time of decomposition (values are mean and SD; for each parameter, data with different letters are significantly different at $p \leq 0.05$).

had significant positive correlations with the salinity and TOM of the sediments (Table 4).

Although the concentration of Cu and Zn increased in the root and leaf litters of *S. alterniflora*, the metal pools in the litters decreased significantly as indicated by the significant decrease of AIs (Fig. 6A and B). At the end of the burial experiment (Day 350), AIs for Cu were 42.9%, 19.3%, and 18.5%, and AIs for Zn were 16.5%, 14.4%, and 4.8%, both for the roots, stems, and leaves, respectively. The changes of Pb-AI in the roots and stems and Cr-AI in the roots and leaves all showed similar patterns with that of Cu and Zn. Moreover, AIs at the end of burial experiment (Day 350) were 14.6%–30.9% and 7.0%–23.5% for Cu and Zn, respectively. Among the different parts of the plant, the leaf had the lowest AI for all of the metals. Notably, the leaf Pb-AI at Day 81 increased to ~258%, and the stem Cr-AI at Day 184 raised to ~197% (Fig. 6C and D). In the litters of the root and leaf, the remains of metals (AI) had significant positive linear relationships with mass remains at different burial stages (Fig. 7A and C). In stem litters, the linear relationship was not significant for Cr (Fig. 7B).

Table 2
Correlation coefficient showing relationships between the decomposition rate of *S. alterniflora* and the C/N ratio, lignin and cellulose content (* and ** indicate the r values are significant at $p \leq 0.05$ and 0.01 levels (2-tailed), respectively).

	Lignin	C/N ratio	Cellulose
Root	−0.561	0.802**	0.640*
Stem	−0.181	−0.036	0.039
Leaf	−0.774**	0.941**	0.019

3.4. Changes of Pb isotope ratio

The ratios of $^{207}Pb/^{206}Pb$ and $^{208}Pb/^{206}Pb$ in root litters decreased significantly with the increasing of burial time until Day 290 (Fig. 8A and B). Moreover, the ratios were lower than their initial values at Days 184 and 290 (shown as negative values in Fig. 8C and D). At Day 350, a significant increase was observed in the ratios of $^{207}Pb/^{206}Pb$ and $^{208}Pb/^{206}Pb$ in the root litters. In comparison, the variation of Pb isotope ratios in the sediment was not significant throughout the entire burial period.

4. Discussion

In the present study, the exponential break down rates (k-value) of different parts of *S. alterniflora* were normally in the range of 0.002–0.020 day^{-1}, which were more or less comparable with these of the other marsh plants in previous studies (Simões et al., 2011; Balasubramanian et al., 2012; Zhang et al., 2014a; Sun et al., 2016) (Table S1 in the supplementary material). In general, litter decomposition can be mainly divided into fast-early and slow-late stages (De Santo et al., 2009; Preston et al., 2009). In the present study, the decay of the leaf litters was rapid during the early stage of the decomposition, approximately 45.9%–53.8% of the leaf dry mass lost at the first 81 days of the decomposition (Fig. 3). The mass loss rate of the root and leaf litters of *S. alterniflora* decreased with the increase of burial time. Notably, Day 81 (25 March) to Day 184 (8 July) covered the seasons of spring and summer, at which the tidal flat sediments had better water and heat conditions compared with that at autumn (Day 290) and winter (Day 350). This condition promotes the growth and propagation of microorganisms in sediments and increased the decomposition of plant litters. At the latter stages, the decomposition rate slowed down obviously due to the increase in the lignin content (Fig. 4).

C/N ratio represents the ratio of carbohydrate and recalcitrant organic fractions (such as lignin and cellulose) to N fractions in litters, and has been used as an effective index of decomposition rate of litters (Dolinar et al., 2016; Sun et al., 2016). The decomposition rate of litter is usually positively correlated with the initial N concentration and negatively correlated with the C/N ratio of litter (Simões et al., 2011; Mohammed et al., 2013). In the present study, the leaf of *S. alterniflora* had significantly lower C/N ratio than that of the root and stem, which made its decomposition rate the highest among the three plant parts. The C/N ratio of *S. alterniflora* peaked on March 25 (Day 80), which was coincided with the time that the greatest litter mass loss was observed. Similar results were also found by Zhang et al. (2014a) that the C/N ratio in leaf litters of *S. alterniflora* increased during the first 90 days of decomposition, followed by a marked decline. The high initial N concentration and low initial C/N ratio may facilitate N loss from the leaf at early stages of decomposition. This phenomenon accounts for the significant increase of C/N ratios in the leaves at early stages of decomposition. The mass loss rate and C/N ratio of the roots and leaves of *S. alterniflora* decreased with increasing burial time, whereas the lignin content increased with increasing burial time. Correlation analysis

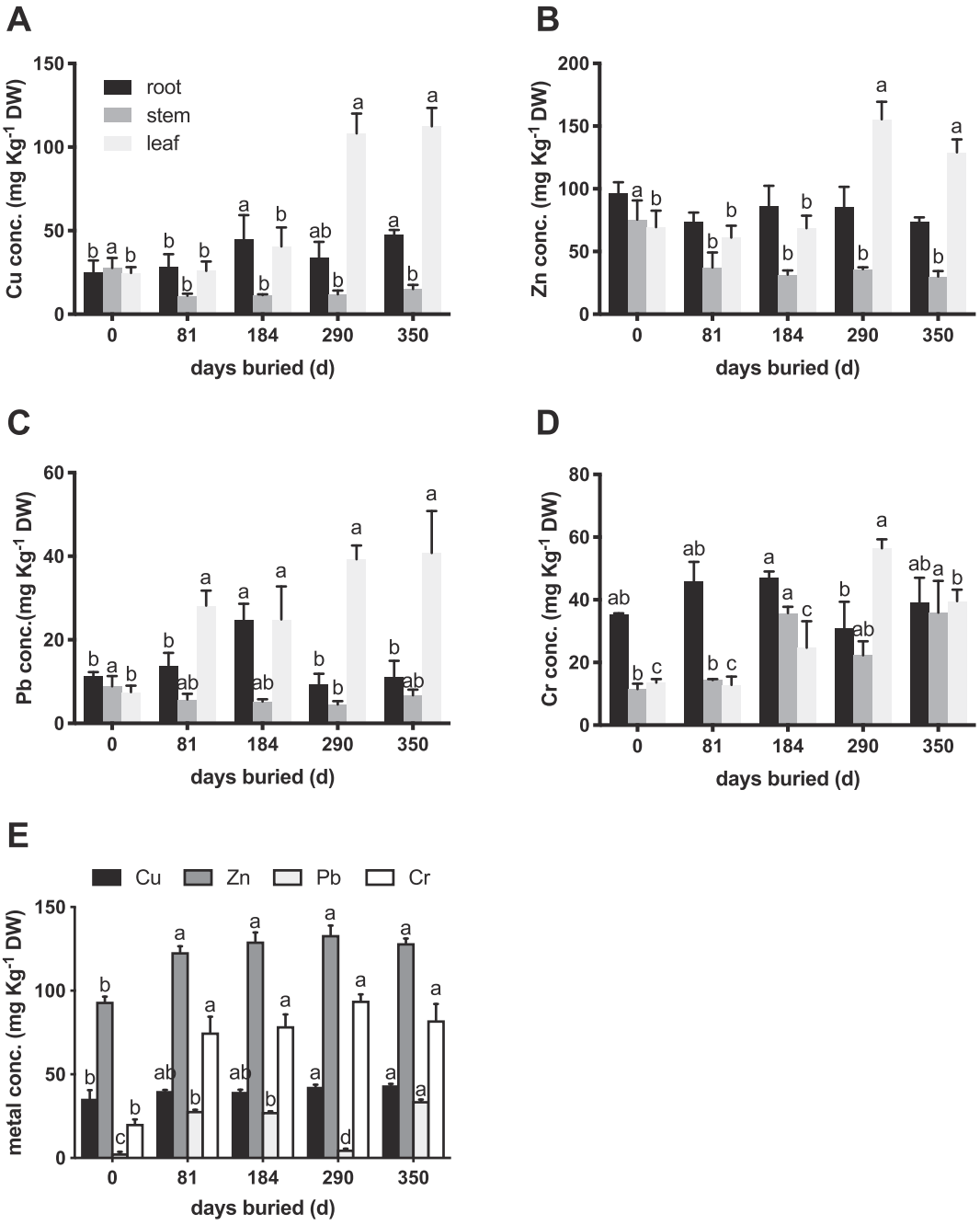

Fig. 5. Concentration of (A) Cu, (B) Zn, (C) Pb and (D) Cr in litters of different part of *S. alterniflora* at different time of decomposition (values are mean and SD; for each plant part, data with different letters are significantly different at $p \leq 0.05$).

also showed a significant positive correlation between the mass loss rate and C/N ratio in the roots and leaves of *S. alterniflora*. The increase in C/N ratio at latter decomposition stages may be associated with increasing lignin proportion in the remaining litter. These results are consistent with most of the previous studies (Preston et al., 2009; Zhang et al., 2014a, 2014b; Sun et al., 2016; Xu et al., 2017). In addition to C/N stoichiometry, the relative composition of organic C (O-alkyl C, di-O-alkyl, aromatic C, etc.) in controlling the decomposition of plants

Table 3
Changes of sediment physiochemical properties in the middle marsh of the tidal flat at different sampling time (In each column, data with different superscript letters indicate the data were significantly different at $p \leq 0.05$; nd, not determined due to the malfunction of the instrument).

Date	Salinity (‰)	TOM (%)	MD (μm)	Eh (mV)	Clay (%)	Silt (%)	Sand (%)
4 Jan (Day 0)	3.2 ± 0.1^{c}	5.3 ± 0.3^{c}	10.5 ± 1.6^{a}	nd	27.5 ± 2.2^{c}	69.4 ± 2.4^{a}	3.1 ± 0.4^{b}
25 Mar (Day 81)	5.0 ± 0.6^{ab}	8.4 ± 0.6^{ab}	6.1 ± 0.5^{b}	nd	37.5 ± 2.1^{a}	58.8 ± 1.0^{b}	3.7 ± 1.5^{b}
8 Jul (Day 184)	3.7 ± 0.4^{c}	7.9 ± 0.4^{bc}	5.8 ± 0.1^{b}	nd	38.2 ± 0.2^{a}	58.3 ± 1.0^{bc}	3.5 ± 0.9^{b}
26 Oct (Day 290)	4.0 ± 0.2^{bc}	11.3 ± 2.3^{a}	8.1 ± 1.3^{ab}	30.3 ± 5.0	31.1 ± 2.7^{b}	54.6 ± 2.0^{c}	14.3 ± 4.5^{a}
23 Dec (Day 350)	5.3 ± 0.5^{a}	10.3 ± 0.3^{ab}	6.8 ± 0.6^{b}	462.0 ± 5.9	34.4 ± 1.8^{ab}	56.7 ± 0.4^{bc}	8.9 ± 1.5^{ab}

Table 4
Correlation coefficient showing relationships between HMs concentration and physiochemical properties of the sediments (* and ** indicate the r values are significant at $p \leq 0.05$ and 0.01 levels (2-tailed), respectively).

Metals	Salinity	TOM	MD	Clay	Silt	Sand
Cu	0.534*	0.750**	−0.498	0.356	−0.755**	0.521*
Zn	0.489	0.754**	−0.686**	0.596*	−0.962**	0.532*
Pb	0.713**	0.224	−0.773**	0.793**	−0.441	−0.233
Cr	0.529*	0.802**	−0.676**	0.576*	−0.961**	0.550*

has also been highlighted by other studies (Xu et al., 2017; Cao et al., 2018). This may provide insights for future study in the decomposition of *S. alterniflora*.

Mineralization, leaching, and erosion are important factors influencing plant litter decomposition in coastal wetlands (Zhao et al., 2015). Periodic tidal flooding is the typical characteristic of tidal flat wetland. With the increase of tidal flat elevation, flood time is often decreased, and vice versa. In the present study, the mass loss rate of the roots and leaves of *S. alterniflora* is usually higher in the high tidal marsh than that in the low tidal marsh, especially at the late stages of decomposition. The results were in accordance with those of previous studies; the increase of flooded time reduces the decomposition rate of litter through the reduction in the sediment redox potential, thereby decreasing the porewater dissolved O_2 concentration and the inhabitation on the activity of sediment microorganisms (Freeman et al., 2004; Laiho et al., 2004). Alternation of dry and wet conditions favors the occurrence of oxic conditions, which stimulate the most efficient aerobic microbial metabolism, thereby accelerating the decomposition of litters (Battle and Golladay, 2001; Anderson and Smith, 2002). Our finding is contrary to several previous studies which found the length of tidal flooding time accelerated the litter decomposition (Liu et al., 2010; Simões et al., 2011; Sun et al., 2012; Zhao et al., 2015; Dolinar et al., 2016). These discrepancies may be induced by the different ways to place the litter bag in the experiments. In our study, the litter bags were covered by approximately 5 cm sediments, whereas in the abovementioned studies, the litter bags were placed on the surface of the marsh sediment, in which tidal flushing exerts direct influences on the breakdown of litters. In addition, fine decomposing materials in the litter bags leach faster due to frequent water-level fluctuations than those under conditions without tidal flushing (Simões et al., 2011; Dolinar et al., 2016).

In the present study, the concentrations of metals (Cu, Zn, Pb, and Cr) in leaf litter of *S. alterniflora* increased significantly during the decomposition, and the metal levels in leaf litters eventually exceeded the levels in sediment (Fig. 5). This result is consistent with many previous reports that metal (such as Cd, Cr, Cu, Ni, Pb, and Zn) concentration increased rapidly in the litters of *Spartina foliosa* (Zawislanski et al., 2001), *S. alterniflora* (Windham et al., 2004), *P. australis* (Windham et al., 2004; Du Laing et al., 2006) and *Potamogeton crispus* during decomposition (Deng et al., 2016). The concentration of Cu, Zn, Pb, and Cr in leaf litters showed similar changes, indicating that they might undergo a similar biogeochemical process during the decomposition (Deng et al., 2016). Previous study showed that the accumulation of metals in the *S. alterniflora* was mainly found in the root, and rarely in the aerial part (especially the leaf) (Windham et al., 2004; Xu et al., 2018). Concentrating of metals, adsorption and microbial action were possibly the major reasons for the enrichment of metals in the leaf litters. In this study, the concentration of metals (especially Cu, Zn and Pb) in leaf litters at the latter stages of decomposition was much higher than that in root litters and adjacent sediments. The significant increase of metal concentration in leaf litters was possibly induced by the concentrating effect which was caused by the rapid loss of leaf mass at the early decomposition stage (Breteler et al., 1981). Besides, as our

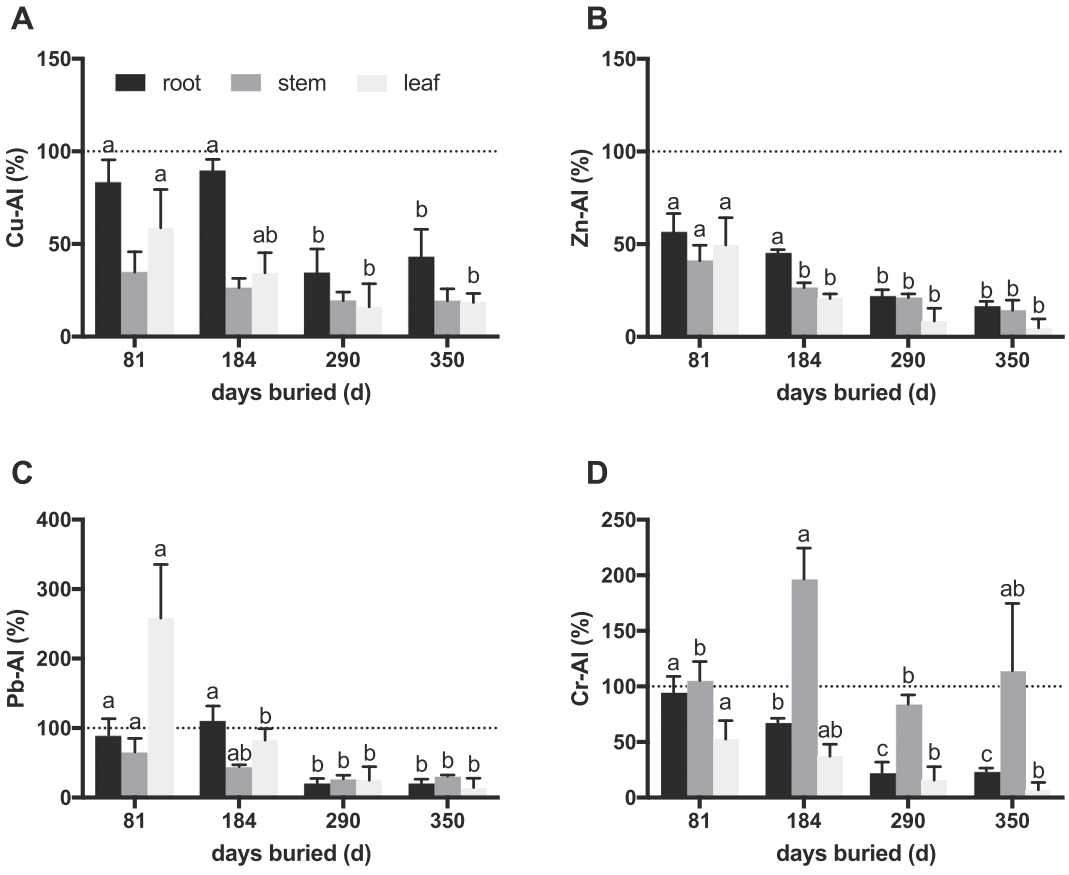

Fig. 6. Accumulation index (AI) of (A) Cu, (B) Zn, (C) Pb and (D) Cr in litters of different part of *S. alterniflora* at different time of decomposition (values are mean and SD; for each plant part, data with different letters are significantly different at $p \leq 0.05$).

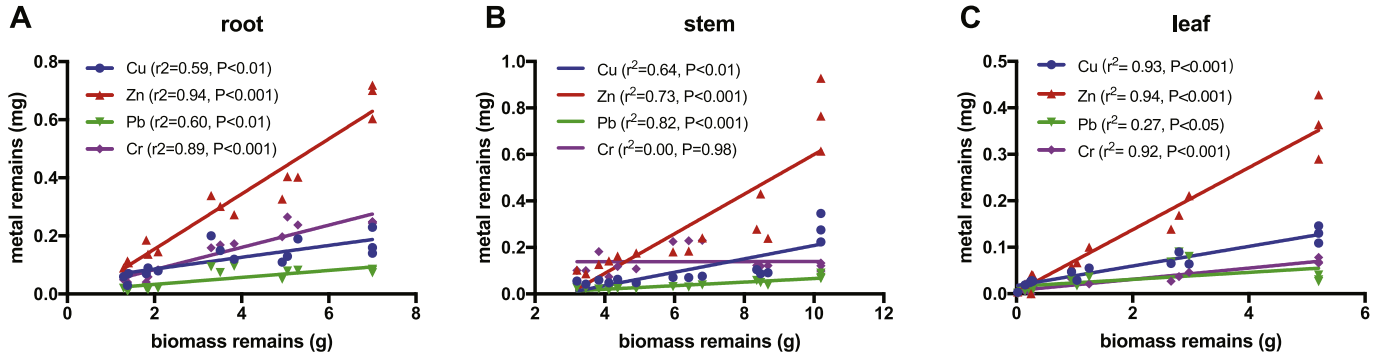

Fig. 7. Linear regressions between the remaining metal stocks and remaining litter biomass of different parts of *S. alterniflora* at different time of decomposition.

litterbags were buried in the anoxic sediments, the plant litter have a lot of sulfide-producing bacteria which can couple the oxidation of organic compounds with the reduction of metals. Therefore, the metal concentration in leaf litters was greatly increased (Windham et al., 2004). Previous studies also found that the biofilm (formed by microbes and their exudates) developed during the decomposition could also contribute to the enrichment of metals in the plant litter (Schaller et al., 2010, 2011). In addition to the above-mentioned reasons, the considerably increased metal concentration in the sediment during the burial experiment (Fig. 5E) also contributed to the enrichment of metals in litters.

The metal enrichment in litters during the decomposition was observed to vary with the metal type and the plant parts (Windham et al., 2004). In the current study, during the decomposition the concentration of Cu and Zn increased significantly in the leaves while decreased significantly in the roots. This synchronous mode of change was due to the fact that Cu and Zn have similar geochemical behaviors and are highly correlated in soil and sediment (Deng et al., 2016). The change pattern of metal concentration in the root litters of *S. alterniflora* was different from that in the leaf, which can be explained by the different breakdown patterns of the two parts (Windham et al., 2004). These metal- and tissue-specific variation of the metal concentration in litters was also found in other marsh plants, such as *P. australis* (Sun et al., 2016), *S. salsa* (Sun et al., 2016, 2017), and *Potamogeton crispus* (Deng et al., 2016). Various influencing factors, such as the utilization of metals by the microbes, the specific adsorption and desorption behavior of the metals in litters, the interactions of the metals with the sediment organic matters, and the tidal wave action, may account for this phenomenon (Sun et al., 2016; Deng et al., 2016). The pools of metals (as indicated by AI in Fig. 6) in the litters decreased significantly with increasing degradation time. Linear regression

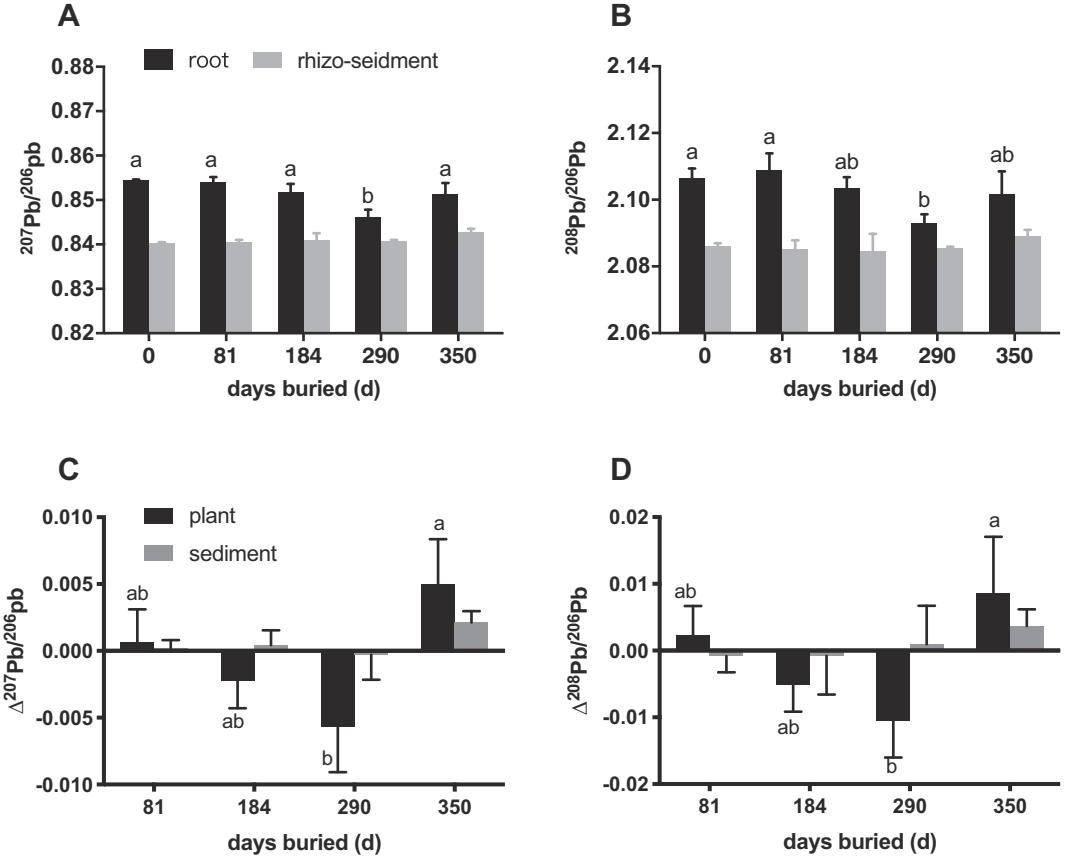

Fig. 8. Changes of root Pb isotope ratios (A) $^{207}Pb/^{206}Pb$ and (B) $^{208}Pb/^{206}Pb$ and relative changes of (C) $^{207}Pb/^{206}Pb$ and (D) $^{208}Pb/^{206}Pb$ compare to their initial values (values are mean and SD; for each parameter, data with different letters are significantly different at $p \leq 0.05$).

analysis showed significant positive correlations between the pools of metals in the litter and the mass loss of litter in each part during decomposition (Fig. 7). The decrease in metal pools might be induced mainly by the mass loss during the decay of plant litters. Similar results were also obtained in decomposition studies of *S. alterniflora* (Windham et al., 2004) and *P. australis* (Windham et al., 2004; Du Laing et al., 2006). The AI values of Cu and Zn in leaf litters were in accordance to the mass loss ratios of the litters at Day 81 (Fig. 3), which indicated the decrease in Cu and Zn pools in leaf litter were mainly due to the rapid mass loss at the early stage of decomposition. Although metals might be accumulated in the plant litter through adsorption and microbial action, the release of the metals through the mass loss could not be counterbalanced. On the other hand, Cu and Zn are the micro-nutrients for the growth of microbes, their consumption by the microbes could also lead to the decrease of AIs.

Pb-AI of leaf litters at Day 81 (25 March) was 258%, indicating that the Pb pool in leaf litters was approximately 2.6 times of the initial value. The high AI of Pb in leaf litters indicating that Pb may be absorbed from the adjacent sediment into litter at the beginning of the decomposition. In the root litters, AI of Pb decreased significantly from Day 184 to Day 290, and the value showed no further change until the end of the burial experiments (Day 350) (Fig. 6). Meanwhile, the Pb concentration in root litters did not change from Day 290 to Day 350, indicating that the release and incorporation of Pb in the root litters were roughly balanced at the late stages of decomposition. The fine scale exchange of Pb between the root litters and the sediments was revealed by the variation of Pb isotope ratios during decomposition. After burying of the root litters, the ratios of $^{207}Pb/^{206}Pb$ and $^{208}Pb/^{206}Pb$ decreased significantly until Day 290 (October 26) and then increased significantly at Day 350 (December 23). However, the change of the two isotope ratios in the sediments did not show any significant variation. These results indicate that Pb in the root litters of *S. alterniflora* was positively output to sediments in the first 290 days of decomposition caused by the mass loss of the root litters because the majority of the root litter mass was lost (approximately 75% as seen in Fig. 3) during this period. The adsorption and desorption of Pb in the marsh sediments can be influenced either by iron cycling or organic matter degradation (Sundby et al., 2005). Pb is prone to adsorption to Fe-oxide and organic matters, and its mobilization in decomposing litters might be enhanced because of Fe-oxide reduction (Sun et al., 2016). This phenomenon accelerated the Pb release in the root litters during the first 290 days of decomposition. The significant increase in Pb isotope ratios on Day 350 indicated that the release of Pb in the plant tissue was greatly inhibited, which can be attributed to i) the slowed mass loss of root litters during this stage, and ii) the retarded Pb release in root litters as a result of the considerable increase of redox potential in the adjacent sediments (Table 3). The incorporation of sediment Pb with low Pb isotope ratios at this stage might overbalanced the release of Pb in the root litters, thereby relatively increasing the Pb isotope ratios in root litters.

5. Conclusions

The present study revealed that the mass loss rate of the root and leaf litters of *S. alterniflora* decreased with the increase of burial time. Leaf had the highest decomposition rate possibly due to the significantly lower C/N ratio compare to that of the roots and stems. Due to the significantly increasing in the lignin content, the decomposition rate of the litters was obviously slowed down at the latter stages of the decomposition. In the present study, the mass loss rate of the roots and leaves of *S. alterniflora* is usually higher in the high tidal marsh than that in the low tidal marsh, especially at the late stages of decomposition. The changes of the metal concentrations in the litters varied with metal types and plant parts. The concentrations of Cu, Zn, Pb, and Cr in leaf litter of *S. alterniflora* increased with the increasing of decomposition time. Nevertheless, the pools of metals in all plant litters decreased significantly with increasing degradation time. The decrease in metal pools possibly be induced by the mass loss during the decay of plant litters, and this was further evidenced by the significantly decreased Pb isotope ratios in root litters and the unaltered Pb isotope ratios in adjacent sediments during decomposition.

Supplementary data to this article can be found online at https://doi.org/10.1016/j.scitotenv.2019.01.422.

Acknowledgement

The work described in this paper was supported by Natural Science Foundation of Shanghai (16ZR1410300), The National Key R&D Program of China (2017YFC0506000), National Natural Science Foundation of China (41877413) and Independent Research Foundation of State Key Laboratory of Estuarine and Coastal Research (2016RCPY01).

References

Anderson, J.T., Smith, L.M., 2002. The effect of flooding regimes on decomposition of polygonum pensylvanicum, in playa wetlands (southern great plains, USA). Aquat. Bot. 74 (2), 97–108.
Balasubramanian, D., Arunachalam, K., Das, A.K., Arunachalam, A., 2012. Decomposition and nutrient release of *Eichhornia crassipes* (Mart.) Solms. under different trophic conditions in wetlands of eastern Himalayan foothills. Ecol. Eng. 44, 111–122.
Battle, J.M., Golladay, S.W., 2001. Hydroperiod influence on breakdown of leaf litter in cypress-gum wetlands. Am. Midl. Nat. 146 (1), 128–145.
Breteler, R.J., Teal, J.M., Giblin, A.E., Valiela, I., 1981. Trace element enrichments in decomposing litter of *Spartina alterniflora*. Aquat. Bot. 11, 111–120.
Caetano, M., Fonseca, N., Cesário, C.V.R., 2007. Mobility of Pb in salt marshes recorded by total content and stable isotopic signature. Sci. Total Environ. 380 (1), 84–92.
Cao, C., Liu, S., Ma, Z., Lin, Y., Su, Q., Chen, H., Wang, J., 2018. Dynamics of multiple elements in fast decomposing vegetable residues. Sci. Total Environ. 616–617, 614–621.
De Santo, A.V., De Marco, A., Fierro, A., Berg, B., Rutigliano, F.A., 2009. Factors regulating litter mass loss and lignin degradation in late decomposition stages. Plant Soil 318 (1–2), 217–228.
Deng, H., Zhang, J., Chen, S., Yang, L., Wang, D., Yu, S., 2016. Metal release/accumulation during the decomposition of *Potamogeton crispus* in a shallow macrophytic lake. J. Environ. Sci. 42, 71–78.
Dolinar, N., Regvar, M., Abram, D., Gaberščik, A., 2016. Water-level fluctuations as a driver of *Phragmites australis* primary productivity, litter decomposition, and fungal root colonisation in an intermittent wetland. Hydrobiologia 774 (1), 69–80.
Du Laing, G., Van Ryckegem, G., Tack, F.M.G., Verloo, M.G., 2006. Metal accumulation in intertidal litter through decomposition leaf blades, sheaths and stems of *Phragmites australis*. Chemosphere 63, 1815–1823.
Du Laing, G., Rinklebe, J., Vandecasteele, B., Meers, E., Tack, F.M.G., 2009. Trace metal behaviour in estuarine and riverine floodplain soils and sediments: a review. Sci. Total Environ. 407 (13), 3972–3985.
Freeman, C., Ostle, N.J., Fenner, N., Kang, H., 2004. A regulatory role for phenol oxidase during decomposition in peatlands. Soil Biol. Biochem. 36 (10), 1663–1667.
Gadd, G.M., 1993. Interactions of fungi with toxic metals. New Phytol. 124 (1), 25–60.
Gingerich, R.T., Merovich, G., Anderson, J.T., 2014. Influence of environmental parameters on litter decomposition in wetlands in West Virginia, USA. J. Freshw. Ecol. 29 (4), 535–549.
Guo, X., Lu, X., Tong, S., Dai, G., 2008. Influence of environment and substrate quality on the decomposition of wetland plant root in the Sanjiang Plain, Northeast China. J. Environ. Sci. 20 (12), 1445–1452.
Heiri, O., Lotter, A.F., Lemcke, G., 2001. Loss on ignition as a method for estimating organic and carbonate content in sediments: reproducibility and comparability of results. J. Paleolimnol. 25, 101–110.
Idaszkin, Y.L., Bouza, P.J., Marinho, C.H., Gil, M.N., 2014. Trace metal concentrations in *Spartina densiflora* and associated soil from a patagonian salt marsh. Mar. Pollut. Bull. 89 (1–2), 444–450.
Laiho, R., Laine, J., Trettin, C.C., Finer, L., 2004. Scots pine litter decomposition along drainage succession and soil nutrient gradients in peatland forests, and the effects of interannual weather variation. Soil Biol. Biochem. 36 (7), 1095–1109.
Ledin, M., 2000. Accumulation of metals by microorganisms processes and importance for soil systems. Earth Sci. Rev. 51 (1), 1–31.
Li, B., Liao, C.H., Zhang, X.D., Chen, H.L., Wang, Q., Chen, Z.Y., Gan, X.J., Wu, J.H., Zhao, B., Ma, Z.J., Cheng, X.L., 2009. *Spartina alterniflora* invasions in the Yangtze River estuary, China: an overview of current status and ecosystem effects. Ecol. Eng. 35, 511–520.
Liao, C., Luo, Y., Jiang, L., Zhou, X., Wu, X., Fang, C., Chen, J., Li, B., 2007. Invasion of *Spartina alterniflora* enhanced ecosystem carbon and nitrogen stocks in the Yangtze Estuary, China. Ecosystems 10 (8), 1351–1361.
Lisamarie, W., Weis, J.S., Peddrick, W., 2010. Metal dynamics of plant litter of *Spartina alterniflora* and *Phragmites australis* in metal-contaminated salt marshes. Part 1: patterns of decomposition and metal uptake. Environ. Toxicol. Chem. 23 (6), 1520–1528.
Liu, P., Wang, Q., Bai, J., Gao, H., Huang, L., Xiao, R., 2010. Decomposition and return of C and N of plant Litter of *Phragmites australis* and *Suaeda salsa* in typical wetlands of the Yellow River Delta, China. Procedia Environ. Sci. 2, 1717–1726.
Lu, W., Liu, N., Zhang, Y., Zhou, J., Guo, Y., Yang, X., 2017. Impact of vegetation community on litter decomposition: evidence from a reciprocal transplant study with ^{13}C labeled plant litter. Soil Biol. Biochem. 112, 248–257.

Mohammed, A.M., Nartey, E., Naab, J.B., Adiku, S.G.K., 2013. A simple model for predicting plant residue decomposition based upon their C/N ratio and soil water content. Afr. J. Agric. Res. 8, 2153–2159.
Niu, S., Zhou, Y., Jiang, H., 1992. Crop Quality Analysis. Agricultural Press, Beijing, China.
Notten, M.J.M., Walraven, N., Beets, C.J., Vroon, P., Rozema, J., Aerts, R., 2008. Investigating the origin of Pb pollution in a terrestrial soil–plant–snail food chain by means of Pb isotope ratios. Appl. Geochem. 23 (6), 1581–1593.
Olson, J.S., 1963. Energy storage and the balance of producers and decomposers in ecological systems. Ecology 44 (2), 322–331.
Preston, C.M., Nault, J.R., Trofymow, J.A., Smyth, C., CIDET Working Group, 2009. Chemical changes during 6 years of decomposition of 11 litters in some Canadian forest sites. Part 1. Elemental composition, tannins, phenolics, and proximate fractions. Ecosystems 12 (7), 1053–1077.
Schaller, J., Weiske, A., Mkandawire, M., Dudel, E.G., 2010. Invertebrates control metals and arsenic sequestration as ecosystem engineers. Chemosphere 79, 169–173.
Schaller, J., Brackhage, C., Mkandawire, M., Dudel, E.G., 2011. Metal/metalloid accumulation/remobilization during aquatic litter decomposition in freshwater: a review. Sci. Total Environ. 409, 4891–4898.
Simões, M.P., Calado, M.D.L., Madeira, M., Gazarini, L.C., 2011. Decomposition and nutrient release in halophytes of a Mediterranean salt marsh. Aquat. Bot. 94 (3), 119–126.
Sun, Z., Mou, X., Liu, J.S., 2012. Effects of flooding regimes on the decomposition and nutrient dynamics of *Calamagrostis angustifolia* litter in the Sanjiang Plain of China. Environ. Earth Sci. 66 (8), 2235–2246.
Sun, Z., Mou, X., Sun, W., 2016. Decomposition and heavy metal variations of the typical halophyte litters in coastal marshes of the Yellow River estuary, China. Chemosphere 147, 163–172.
Sun, Z., Mou, X., Zhang, D., Sun, W., Hu, X., Tian, L., 2017. Impacts of burial by sediment on decomposition and heavy metal concentrations of *Suaeda salsa* in intertidal zone of the Yellow River estuary, China. Mar. Pollut. Bull. 116 (1–2), 103–112.
Sundby, B., Caetano, M., Vale, C., Gobeil, C., Nuzzio, D.B., 2005. Root-induced cycling of lead in salt marsh sediments. Environ. Sci. Technol. 39 (7), 2080–2086.
Syros, T., Yupsanis, T., Zafiriadis, H., Economou, A., 2004. Activity and isoforms of peroxidases, lignin and anatomy, during adventitious rooting in cuttings of *Ebenus cretica*, L. J. Plant Physiol. 161 (1), 69–77.
Weis, J.S., Weis, P., 2004. Metal uptake, transport and release by wetland plants: implications for phytoremediation and restoration. Environ. Int. 30, 685–700.
Windham, L., Weis, J.S., Weis, P., 2004. Metal dynamics of plant litter of *Spartina alterniflora* and *Phragmites australis* in metal-contaminated salt marshes. Part 1: patterns of decomposition and metal uptake. Environ. Toxicol. Chem. 23 (6), 1520–1528.
Xu, Y., Chen, Z., Fontaine, S., Wang, W., Luo, J., Fan, J., Ding, W., 2017. Dominant effects of organic carbon chemistry on decomposition dynamics of crop residues in a Mollisol. Soil Biol. Biochem. 115, 221–232.
Xu, Y., Sun, X., Zhang, Q., Li, X., Yan, Z., 2018. Iron plaque formation and heavy metal uptake in *Spartina alterniflora* at different tidal levels and waterlogging conditions. Ecotoxicol. Environ. Saf. 153, 91–100.
Yang, H., Linge, K., Rose, N., 2007. The Pb pollution fingerprint at lochnagar: the historical record and current status of Pb isotopes. Environ. Pollut. 145 (3), 723–729.
Young, S.D., 2013. Chemistry of heavy metals and metalloids in soils. In: Brian, J.A. (Ed.), Heavy Metals in Soils. Springer, Dordrecht, pp. 51–95.
Zawislanski, P.T., Chau, S., Mountford, H., Wong, H.C., Sears, T.C., 2001. Accumulation of selenium and trace metals on plant litter in a tidal marsh. Estuar. Coast. Shelf Sci. 52 (5), 589–603.
Zhang, L.H., Tong, C., Marrs, R., Wang, T.E., Zhang, W.J., Zeng, C.S., 2014a. Comparing litter dynamics of *Phragmites australis* and *Spartina alterniflora* in a sub-tropical Chinese estuary: contrasts in early and late decomposition. Aquat. Bot. 117, 1–11.
Zhang, X., Song, C., Mao, R., Yang, G., Tao, B., Shi, F., Zhu, X., Hou, A., 2014b. Litter mass loss and nutrient dynamics of four emergent macrophytes during aerial decomposition in freshwater marshes of the Sanjiang plain, Northeast China. Plant Soil 385 (1–2), 139–147.
Zhao, Q., Bai, J., Liu, P., Gao, H., Wang, J., 2015. Decomposition and carbon and nitrogen dynamics of *Phragmites australis* litter as affected by flooding periods in coastal wetlands. CLEAN–Soil Air Water. 43, pp. 441–445.